ELSEVIER

Bone Vol. 17, No. 3
September 1995:229–237

Evidence of Strain-Mode-Related Cortical Adaptation in the Diaphysis of the Horse Radius

M. W. MASON, J. G. SKEDROS, and R. D. BLOEBAUM

Bone and Joint Research Laboratories, V.A. Medical Center, and Division of Orthopedic Surgery, University of Utah School of Medicine, Salt Lake City, UT, USA

The relative importance that certain strain features, including mode (e.g., tension vs. compression) and magnitude, have in affecting adaptive bone remodeling seen in normal skeletally mature bones remains controversial. The equine radius is used as a model because in vivo strain data show that the mid-to-proximal diaphysis receives a consistent history of predominantly cranial-caudal bending loads, in contrast to the distal diaphysis which receives relatively more torsional loading superimposed on cranial-caudal bending. Medial and lateral cortices serve as control regions because they correspond to a neutral axis of bending. Equine radii were sectioned transversely at 65% (proximal), 50%, and 35% (distal) of length and cortical bone from the cranial ("tension"), caudal ("compression"), medial, and lateral regions was examined to determine if one, of many, structural and material features could be distinguished as being consistently related to the distribution of the prevailing strain modes. Mineral content (percent ash) differences, though statistically significant ($p < 0.01$), vary less than 1% between regions of the cortex at all sections. Porosity is not significantly different between any of the regions ($p = 0.13$). In the 65% and 50% sections, secondary osteon population density (OPD, osteons per square millimeter) and fractional area of secondary bone (FASB) are each nearly two times as great in the caudal regions than in the other three regions ($p < 0.01$). The 35% section shows a pattern opposite of that in the other sections—there are more than two times as many osteons in the *cranial* cortex than in the caudal cortex. However, at all section locations, collagen fibers have more oblique-to-transverse orientation in the caudal cortex and have relatively more longitudinal orientation in the cranial cortex ($p < 0.01$). Collagen fiber orientation is not significantly different between medial and lateral cortices at any section location ($p > 0.3$). Because the caudal cortex of the 35% section is significantly less remodeled (lower OPD and FASB) than the opposite cranial cortex, the oblique-to-transverse collagen seen in the caudal cortex of this section cannot be attributed to prior remodeling activity. These data show that the greatest amount of remodeled bone does not consistently occur in the caudal cortex, where strain magnitudes are invariably greatest. However, collagen fiber orientation is markedly different between the opposite cortices in a pattern that consistently coincides with the cranial-caudal distribution of bending strains. These data support the hypothesis that the primary bone and/or bone within secondary osteons of the cranial and caudal cortices is organized with some recognition of prevailing strain mode. (*Bone 17:229–237; 1995*)

Key Words: Horse radius; Bone remodeling; Cortical bone adaptation; Osteon; Strain magnitude; Strain mode.

Introduction

The structural and material organization of cortical bone tissue reflects the history of bone cell activity at the local level. Regional differences in cortical bone microstructure, collagen fiber orientation, and mineral content between regions of the same cross-section have led some investigators to suggest that different regions within a normal skeletally mature bone require specific material properties.[33,34,44,45] Regional differences in cortical tissue organization that coincide with regional differences in strain environments within one bone suggest that bone cells have the capacity to directly, or indirectly, sense and respond to mechanical strain.[4,10,18,24,36,38,44,45] However, it remains unclear if the regional structural and material differences that have been described in some bones represent significant functional adaptation to local strain stimuli, or if these findings are simply byproducts of processes that are not strongly influenced by strain-related stimuli.[38,44,45]

Because most bones have complex strain environments, it is not entirely clear which of the many strain features, such as mode (e.g., tension vs. compression), magnitude, rate, and others, if any, are specifically involved in governing the bone cell activities that produce and maintain the structural/material organization of a normal bone.[21,27,38,44,45] Identification of a link between a bone's remodeling history and specific strain features is important in understanding bone organ homeostasis, but is hard to establish because of the difficulty in isolating and observing bone tissue in vivo for long periods of time without creating a pathologic condition or perturbing the normal loading conditions.

Skedros et al.[44,45] suggest that mechanically relevant functional adaptations to a long history of specific strain features, if present, would be most clearly manifest in bones subject to simple loading conditions. Using mule deer calcanei, a simple cantilevered bending system, they showed what they considered to be "strain-mode-specific" microstructural and mineral content differences between tension (caudal) and compression (cranial) cortical regions. However, they suggest that the presence of the

Address for correspondence and reprints: Dr. Roy D. Bloebaum, Bone and Joint Research Laboratories (151F), V.A. Medical Center, 500 Foothill Boulevard, Salt Lake City, UT 84148.

8756-3282/95/$9.50
SSDI 8756-3282(95)00213-W

Bone Vol. 17, No. 3
September 1995:229–237

firmly adherent plantar ligament may affect the underlying tension cortex by stress shielding this region. They were therefore reticent to conclude that the remodeling differences reported were purely strain-mode specific.

The present study further explores the idea that bone organization is influenced by a long history of a consistent distribution of specific strain features, such as mode and magnitude, by examining a tension/compression bone that lacks a firmly adherent load-bearing member. The horse radius overcomes some limitations of the artiodactyl calcaneus model in that the associated soft tissues are not as firmly adherent to adjacent cortical regions, and muscle attachments are absent along the greater part of the diaphysis.[16] Using rosette strain gauges placed at multiple locations, the in vivo mechanical strain environment in the horse radius during various normal gaits has been described.[5,35,41,46] In the proximal and middle portions of the diaphysis, the neutral axis of bending passes in a roughly mediolateral direction through the medullary canal **(Figure 1).** In vivo measurements by Schneider et al.[41] show that at the mid-to-proximal diaphysis of the horse radius the cortex located cranial (anterior) to the medullary canal receives predominantly tension strains with peak magnitudes of approximately 1200 microstrain (mS). The cortex located caudal (posterior) to the medullary canal receives predominantly compression strains with peak magnitudes of approximately −1900 mS. In the 35% section, which is located in the distal diaphysis, the strain environment is more complex, being produced by relatively more prominent torsional loads which coexist with cranial-caudal bending.[41]

The objective of the present study is to extend and clarify our previous work on how the organization of cortical bone of the appendicular skeletons of skeletally mature animals may be related to specific strain features produced during functional loading. We hypothesize that mechanically relevant adaptations to strain mode and/or strain magnitude can be distinguished as structural and/or material differences between tension and compression regions of the mid-to-proximal horse radius, and these adaptations will be less distinct in the distal diaphysis where torsional strains increase the complexity of the strain milieu.

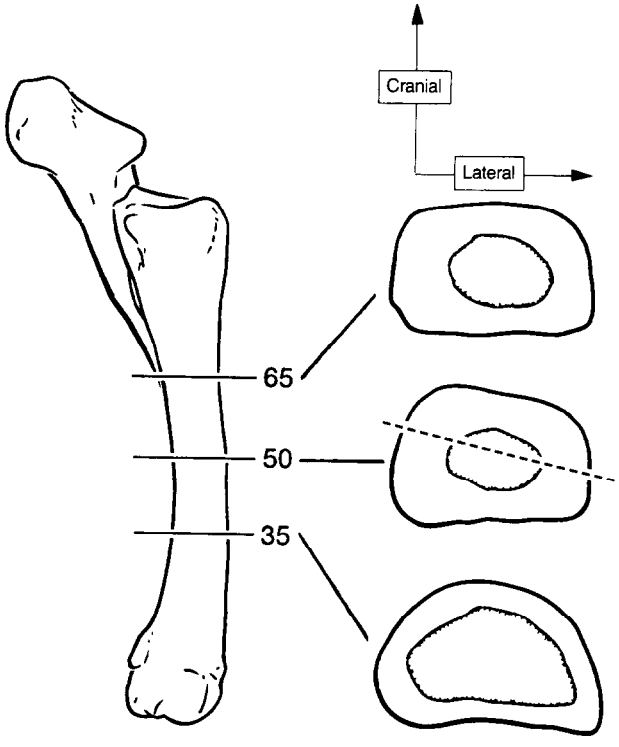

Figure 1. Diagram of the horse radius and representative sections at 35% (distal), 50%, and 65% (proximal) of bone "length." An estimated neutral axis, based on previous strain gauge studies,[41,46] is illustrated on the 50% section.

Methods

One radius was obtained from each of 18 skeletally mature standard breed horses with no evidence of skeletal pathology at the time of death. Each bone was manually cleaned of soft tissue, and sectioned transversely at 35% (distal), 50%, and 65% of length (Figure 1). Two 3-mm-thick sections were taken from each of the three locations. One section from was saved in 70% ethanol at room temperature for the determination of mineral content by ashing. The other section was embedded in polymethyl methacrylate (PMMA),[14] and saved for microstructure and collagen fiber orientation analyses.

Mineral Content

A three-millimeter-wide piece, spanning the entire cortex, was removed from each cortical quadrant (cranial, caudal, medial, lateral) of each section. The pieces were then cut in half so that there were superficial and deep specimens. Using conventional methods[13,43] the pieces were thoroughly defatted in full-strength chloroform, dried to constant weight at 80°C (<0.05% change), and ashed at 600°C for 24 h. Mineral content is expressed as the percentage ratio of the weight of the ash divided by the weight of the dried, defatted bone.

Microstructure

Ten radii were used to quantify cortical microstructure. One PMMA-embedded section from each of the 35%, 50%, and 65% locations was selected for imaging. The distal surface of each embedded section was ground, polished, and prepared for imaging in the backscattered electron mode of the scanning electron microscope.[7,42,43] Two 50× micrographs (7.36 mm^2) were taken within each of the three envelopes of the cranial, caudal, medial, and lateral cortices. The pericortical envelope (P) is located immediately adjacent to the periosteal surface of the bone without including circumferential lamellae. The endocortical envelope (E) is located near the medullary canal without including trabecular bone, or the porous transition zone (described below). The middle envelope (M) is located equidistant between the other two envelopes. In the 50% and 65% sections, the boundary between cortical bone and medullary canal is easily distinguished due to lack of, or small amount of, cancellous bone at these locations. However, the medullary canal at the 35% section was completely filled with cancellous bone. Microscopic examination of the 35% sections revealed a porous transition zone between cortical and cancellous bone; this was excluded from analysis using criteria described by Skedros et al.[45] Using standard stereologic point-counting techniques,[30,40] the micrographs were analyzed for: (1) number of secondary osteons per square millimeter; (2) the fractional cross-sectional area occupied by secondary osteons; (3) the fractional area occupied by porous spaces; (4) the fractional area occupied by resorption spaces; and (5) estimated mean area per osteon.

Osteon Population Density (OPD) (Number of Secondary Osteons per Square Millimeter)

Using criteria of Skedros et al.,[45] the following were counted as osteons: (1) complete secondary osteons; (2) partially formed secondary osteons, in which the entire outer circumference of the preceding resorption space was lined with new bone; and (3) secondary osteon fragments, which had a complete central canal.

Fractional Area of Secondary Bone (FASB)

The fractional area of secondary bone (FASB) is defined as the total area of secondary bone (S) in each envelope (two images) divided by the total area of secondary bone plus interstitial (nonsecondary) bone (I), [S/(S + I)].[45] A 9.5 mm grid (101 ± 4 points per micrograph) was randomly superimposed over each 50× micrograph. Each point was classified as either secondary or nonsecondary bone. Nonsecondary bone included interstitial bone, primary bone, and plexiform bone. The area of secondary bone included the central canal of each secondary osteon. Porosity data (defined below) were collected separately. Because these data showed no differences between cranial and caudal regions, the FASB was not subsequently corrected for porosity.

Porosity

Structures contributing to porosity measurements include central canals of secondary osteons, resorption spaces, and other soft tissue spaces such as Volkmann's canals. Areas occupied by lacunae and canaliculi were not quantified. Porosity measurements were made with a 3.5 mm grid (862 ± 10 points per micrograph) placed over each 50× image.

Estimated Mean Area per Osteon

Area per osteon was estimated by dividing the total cross-sectional area of secondary bone in each image by the number of osteons in each image.

Collagen Fiber Orientation

Using a diamond blade saw (Exact, West Germany), a 1-mm-thick section was obtained from each of the 30 undecalcified PMMA-embedded bulk sections that had been used for microstructural analyses. One surface was ultramilled to a high-luster finish (Reichert/Jung Ultramiller). The milled surface was then mounted with cyanoacrylate glue onto a Plexiglas slide and allowed to cure for 24 h. The opposite side was then milled to achieve an overall uniform thickness of 100 (±5) μm.

According to the method of Boyde and Riggs[10] milled sections were placed between appropriately crossed left and right hand sheets of circular polarizing material (HNCP37 × 0.030-in. filter; Polaroid Corp., Norwood, MA) and analyzed for collagen orientation using circularly polarized light (CPL). Sections were viewed in the light microscope and regional differences in collagen fiber orientation are inferred from corresponding regional differences in the intensity of transmitted light, where darker gray-levels represent more longitudinal collagen and brighter gray-levels represent more oblique-to-transverse collagen.

Using algorithms of a commercially available image analysis system (Image 1, Universal Imaging Corp., West Chester, PA) and a video camera and monitor (Sony Video Camera Model DXC-750MD and Sony Trinitron Color Video Monitor Model PVM-1343MD; Japan), high resolution black and white images (62.5×; approximately 2 mm^2) with a 512 × 480 pixel array and 256 gray-level spectrum were captured directly from the microscope and stored onto disks. Gray-level values (shades of gray) were subsequently quantified in the image taken in each cortical envelope location where microstructural analysis had been done, and ashed samples had been taken in the adjacent proximal sections. Uniformity of the light source was verified periodically, and all images were captured in one continuous imaging session. Because image gray levels remained consistent (<0.05% change), no brightness/contrast calibrations were performed.

Differences in transmitted light intensity, seen on the monitor as differences in image gray-levels, were converted into integer values ranging from 0, 1, 2, . . . 255. For each image, gray-level histograms were constructed after calculating the area fractions of pixels (as a fraction of total pixels) with a discrete gray level. Using the gray-level histograms, a weighted mean gray level (WMGL) was calculated.[9] The darkest gray-levels (0, 1, 2, . . . 6) were eliminated from the calculation of WMGLs, because they represent porous spaces and other tissue voids. Average WMGLs were determined for each cortical envelope and region.

Statistical/Data Analysis

Though all were skeletally mature, the precise ages of the animals were not available. The data were therefore examined for interanimal variations that might be attributable to age, including diffuse increases in porosity and mineral content.[27] Variations in the material organization of cortical bone within the same cross-section are also important considerations because they can be the result of osteon "remodeling drifts" that follow the direction of maturation-related cortical drift, and, therefore, are not necessarily mechanically adaptive.[25,27] Riggs et al.[32] have stated that the cortical bone of the midshaft of the horse radius progressively remodels from caudal to cranial, which, they imply, follows the direction of antecedent cortical drift. (In contrast, observations of Vigliani[47] suggest that drift may occur preferentially *toward* the caudal cortex.) In the context of observations of Riggs et al.,[32] increases in OPD in the cranial cortex occur at a later time than in the caudal cortex since the bone tissue in the cranial cortex is more recently deposited (younger mean tissue age). As the animals age, this remodeling would reduce relative differences in OPD between the opposing cranial and caudal cortices. Increased remodeled bone in the cranial cortex also increases porosity, because the central canals of secondary osteons yield greater porosity than the antecedent primary bone.[27] Consequently, older bones would have smaller differences in porosity between the opposing cortices. Finally, if the bone in the cranial cortices had reached a steady state of remodeling (no net loss or gain of bone mass), and had been in a steady state for a sufficient period of time to complete secondary mineralization,[20] then there would be a slight difference in mineral content between these opposing cortices.

The probability that all of the bones examined in the present study are in a steady state of remodeling is supported by the equal numbers of resorption spaces between opposing cortices. No animal demonstrated any reduction in cranial-caudal differences in OPD or porosity exceeding 2 SD of the mean. Furthermore, no interanimal variations in OPD, porosity, and/or mineral content that can be associated with advanced age were detected. Data were then examined utilizing a three-way ANOVA statistical design. Data were grouped together and compared according to cortex (cranial, caudal, medial, and lateral), cortical envelope (pericortical, middle, endocortical), and section location (35%, 50%, 65% of length). Fisher's LSD test was used to

Bone Vol. 17, No. 3
September 1995:229–237

determine statistical significance of pairwise comparisons. Differences are considered statistically significant when $p < 0.01$. ANOVA results are shown in **Table 1.**

Results

Results are summarized in **Tables 2 and 3** (see also Figure 3). **Figure 2** shows a representative backscattered electron image from the middle envelope of each of four cortices of a 50% section.

Predominate Tension/Compression Environment (50% and 65% Sections Only)

Mineral content (ash fraction). Mineral content in the caudal (compression) (68.0 ± 0.8%) is less than either medial (68.4 ± 1.2%) or lateral (68.8 ± 1.0%) cortices ($p < 0.005$). Also, the cranial (tension) cortex (68.3 ± 1.2%) has less mineral than the lateral cortex (68.8 ± 1.0%) ($p < 0.01$). However, the differences, as noted, are quite small. The cranial cortex (68.3 ± 1.2%) tended to be greater than the caudal cortex (68.0 ± 0.8%) but did not meet the criterion for statistical significance ($p = 0.04$). There is no difference between the cranial cortex and the medial cortex ($p > 0.4$). With all cortices combined, the difference between the 50% (68.2 ± 1.1%) and 65% (68.6 ± 1.1%) sections, though statistically significant ($p < 0.0002$), is also quite small.

Osteon population density (OPD). With data from all envelopes (P, M, and E) in each cortex combined, there are no differences between the cranial cortex (9.4 ± 5.2), medial cortex (8.5 ± 4.7), and lateral cortex (8.3 ± 4.3) ($p = 0.21$). However, the OPD in the caudal cortex (18.1 ± 4.9) is significantly greater than in each of the other cortices ($p < 0.00001$). When grouped by cortical envelope, the data from the caudal cortex show a progressive decrease in OPD from the periosteal to the endosteal surfaces (P = 20.1 ± 3.9; M = 18.9 ± 4.6; E = 15.3 ± 4.9; $p < 0.0102$). A similar decrease is *not* seen in the cranial cortex (P = 8.6 ± 4.4; M = 9.5 ± 5.4; E = 10.1 ± 5.8; $p = 0.38$). Similar to the cranial cortex, the medial ($p < 0.02$) and lateral ($p < 0.09$) cortices also show greater OPD in the endocortical versus the pericortical envelope (Table 2). However the middle cortical envelopes do not differ from either the pericortical or endocortical envelopes (lateral: $p > 0.13$; medial: $p > 0.28$). There is no OPD difference between the 50% and 65% sections (all cortices combined for each section, $p > 0.4$).

Table 1. Results of ANOVA analysis for microstructural and mineral content comparisons

	50% and 65% sections		35% sections	
	Comparison by:	*p* Value	Comparison by:	*p* Value
Mineral content	Quadrant	<0.0001	Cranial section	<0.0001
	Cranial PMD	0.0001	Caudal section	0.0018
	Caudal PME	0.0001		
	Lateral PME	<0.0001		
	Medial PME	<0.0001		
OPD	Quadrant	0.0001	Cranial section	<0.00001
	Cranial PMD	0.53	Caudal section	<0.00001
	Caudal PME	0.0044		
	Lateral PME	0.05		
	Medial PME	0.05		
FASB	Quadrant	<0.0001	Cranial section	<0.00001
	Cranial PMD	0.02	Caudal section	<0.00001
	Caudal PME	0.09		
	Lateral PME	0.01		
	Medial PME	0.23		
Porosity	Quadrant	<0.00001	Cranial section	0.0005
	Cranial PMD	<0.00001	Caudal section	0.9366
	Caudal PME	0.00042		
	Lateral PME	0.0069		
	Medial PME	0.0001		

Cranial = "tension" cortex; caudal = "compression" cortex. OPD = osteon population density; FASB = fractional area of secondary bone; P = pericortical; M = middle; E = endocortical.

Fractional area of secondary bone (FASB). With data from all envelopes (P, M, and E) in each cortex combined, there are no differences in the FASB between the cranial cortex (26.9 ± 15.2%), the medial cortex (26.4 ± 16.8%) and the lateral cortex (24.9 ± 14.5%) ($p > 0.4$). In the caudal cortex (53.7 ± 12.1%), FASB is significantly greater than in each of the other cortices ($p < 0.00001$). In other words, the caudal cortex is more highly remodeled. Within the caudal cortex, the endocortical envelope has a lower FASB (47.6 ± 13.3%) than either the middle (57.0 ± 12.3%, $p = 0.013$) or the pericortical (56.4 ± 8.1%, $p = 0.02$) envelopes. In contrast, in the cranial cortex the endocortical envelope tends to have *higher* FASB (31.4 ± 16.4%) than the middle (25.4 ± 15.1%) and pericortical (23.8 ± 13.7%) envelopes ($p = 0.11$). The medial and lateral cortices also show a pattern of higher FASB in their endocortical envelopes compared to the pericortical envelopes (medial: $p = 0.11$; lateral: $p = 0.006$) (Table 2). There is no difference in FASB between the 50% and 65% sections (all cortices combined for each section, $p = 0.24$).

Porosity. Porosity expressed as percent differences did not differ significantly between caudal (4.9 ± 2.3%), cranial (4.3 ± 2.3%), medial (5.2 ± 2.3%), and lateral (4.9 ± 2.5%) cortices ($p = 0.13$)—with one exception: the medial cortex tended toward a greater porosity than the cranial cortex ($p = 0.03$). Within each cortex, however, significant differences were identified. In the caudal cortex, the endocortical envelope is more porous (6.7 ± 3.1%) than the middle (4.3 ± 1.1%) and the pericortical (3.7 ± 0.8%) envelopes ($p < 0.0005$). A similar pattern is seen in the medial and lateral cortices (Table 2). In the cranial cortex the endocortical envelope (5.7 ± 2.4%) is also more porous than the middle (4.1 ± 2.3%) ($p = 0.03$) and pericortical (3.3 ± 1.4%) ($p < 0.002$) envelopes. Porosity in the middle envelope, however, is not different from the pericortical envelope ($p = 0.28$).

Mean area per osteon. Calculated mean area per osteon is included here to illustrate differences in osteon size that are implied by the reported data (Table 2). Osteons are equally sized between cranial (0.031 mm^2), caudal (0.031 mm^2), medial (0.030 mm^2), and lateral (0.030 mm^2) cortices. In general, osteons in the endocortical envelopes (0.034 mm^2) are larger than in the corresponding middle (0.031 mm^2) and pericortical (0.029 mm^2) envelopes. Mean osteon diameters were calculated assuming a circular cross-sectional shape and are shown in Figure 3d.

Collagen fiber orientation. At the 65% and 50% section locations, the caudal cortex has relatively more oblique-to-transverse collagen fiber orientation, and the cranial cortex more longitudinal collagen fiber orientation. The corresponding differences in WMGL between these opposite cortices are on the order of 50% ($p < 0.01$) (Table 3). Differences in WMGLs between the medial and lateral regions do not significantly differ ($p > 0.3$), which represent near-equivalent collagen fiber orien-

Table 2. Means and standard deviations (SD) for the microstructural data at the 35% (proximal), 50%, and 65% (distal) sections

	Ost/mm²		FASB		Porosity			Ash fraction	
	Mean	(SD)	Mean	(SD)	Mean	(SD)	Area/ost (mean)	Mean	(SD)
50% and 65% sections data combined									
Cranial cortex (tension)								68.3	(1.2)
Pericortical	8.6	(4.5)	23.8	(14.0)	3.3	(1.5)	0.028		
Middle	9.5	(5.5)	25.4	(16.1)	4.1	(2.2)	0.031		
Endocortical	10.1	(5.5)	31.4	(15.5)	5.7	(2.4)	0.037		
Caudal cortex (compression)								68.0	(0.8)
Pericortical	20.1	(4.7)	56.4	(10.2)	3.7	(0.7)	0.030		
Middle	18.9	(4.4)	57.0	(14.3)	4.3	(1.3)	0.030		
Endocortical	15.3	(4.4)	47.6	(11.4)	6.7	(3.2)	0.033		
Medial cortex								68.4	(1.2)
Pericortical	7.2	(4.9)	22.9	(17.0)	3.8	(1.4)	0.030		
Middle	8.3	(5.0)	24.8	(17.8)	5.2	(1.8)	0.030		
Endocortical	9.9	(4.8)	31.7	(17.5)	6.7	(1.8)	0.031		
Lateral cortex								68.8	(1.0)
Pericortical	6.8	(3.4)	18.5	(10.3)	4.0	(2.9)	0.028		
Middle	8.1	(4.3)	24.9	(15.7)	4.5	(1.8)	0.031		
Endocortical	10.1	(4.6)	31.4	(15.3)	6.3	(2.8)	0.033		
35% sections data									
Cranial cortex								66.8	(1.1)
Pericortical	14.2	(5.5)	42.3	(14.4)	3.7	(1.1)	0.031		
Middle	17.1	(5.8)	50.4	(15.4)	3.8	(1.4)	0.031		
Endocortical	13.8	(4.4)	52.7	(15.7)	6.0	(2.8)	0.041		
Caudal cortex								67.2	(1.0)
Pericortical	15.2	(3.8)	46.7	(12.5)	2.7	(0.8)	0.032		
Middle	7.6	(3.9)	29.6	(12.0)	3.2	(1.0)	0.039		
Endocortical	5.5	(2.6)	22.6	(12.4)	3.9	(2.3)	0.049		

Ost/mm² = osteon population density; FASB = fractional area of secondary bone; porosity = fractional area of porous spaces; area = estimated mean area per osteon (micrometers). Fractional areas and ash fractions are expressed as percentages.

tations (Table 3). Examination of the intracortical envelopes shows that collagen fibers have roughly equivalent orientation from the endocortex to the pericortex (50% section: E = 79.3, M = 81.1, P = 89.1 [$p = 0.24$]; 65% section: E = 108.3, M = 110.0, P = 119.2 [$p = 0.25$]).

Combined Tension/Compression and Torsion Environment (35% Sections)

Sections loaded in simple bending (50% and 65%) are compared with sections that have a more complicated strain milieu (35%). Results are summarized in Tables 1–3 and **Figure 3.**

Table 3. Means and standard deviations (SD) for the collagen orientation (WMGL) data

Section	Region	Gray level	(SD)	GL %diff	*p* Value
65%	Cranial	102.34	(27.29)		
	Caudal	150.11	(28.14)	46.7%	<0.00001
	Medial	92.82	(18.02)		
	Lateral	102.32	(39.94)	10.2%	>0.4
50%	Cranial	76.98	(21.89)		
	Caudal	118.50	(37.27)	54.0%	<0.00001
	Medial	71.86	(26.70)		
	Lateral	64.76	(19.79)	11.0%	>0.4
35%	Cranial	107.44	(23.69)		
	Caudal	151.9	(29.50)	41.4%	<0.00001
	Medial	124.74	(23.24)		
	Lateral	122.39	(19.47)	1.9%	>0.4

GL %diff = % gray-level difference of sample means: cranial vs. caudal or medial vs. lateral.

Mineral content (percent ash). The caudal cortex of the 35% sections (67.2 ± 1.0%) has lower mineral content than the caudal (compression) cortex of either 50% (67.9 ± 0.9%) or 65% (68.0 ± 0.7%) sections ($p < 0.003$). The cranial cortex of the 35% sections also has lower mineral content (66.8 ± 1.1%) than the cranial cortex of either the 50% (67.9 ± 1.2%) or the 65% (68.7 ± 1.1%) sections ($p < 0.006$). Though statistically significant, these differences are quite small.

Osteon population density (OPD). In the caudal cortex, OPD in the 35% section (9.4 ± 5.4) was less than either the 50% (18.6 ± 4.5) or the 65% (17.7 ± 5.3) sections ($p < 0.00001$). In the cranial cortex, OPD is greater at the 35% section (15.0 ± 5.3) than at either the 50% (10.3 ± 5.1) or the 65% (8.5 ± 5.1) sections ($p < 0.0008$). In contrast to the 65% and 50% section, these data show that in the *cranial* cortex of the 35% section the OPD is approximately two times *greater* than in the caudal cortex.

Fractional area of the secondary bone (FASB). The FASB in the caudal cortex of the 35% sections (33.0 ± 16.5%) is less than either the 50% (54.9 ± 8.6%) or 65% (52.5 ± 14.8%) sections ($p < 0.00001$). However, in the cranial cortex, the FASB in the 35% section (48.5 ± 14.4%) is *greater* than in the 50% section (28.5 ± 14.9%) and the 65% section (25.2 ± 15.6%) ($p < 0.00001$).

Porosity. The caudal cortex of the 35% sections is less porous (3.3 ± 1.6%) than either the 50% (5.2 ± 2.5%) or the 65% (4.6 ± 2.1%) sections ($p < 0.006$). This difference can be attributed to differences between the endocortical envelopes of these sections. In the cranial cortex, porosities in the 35% sections (4.5 ±

Bone Vol. 17, No. 3
September 1995:229–237

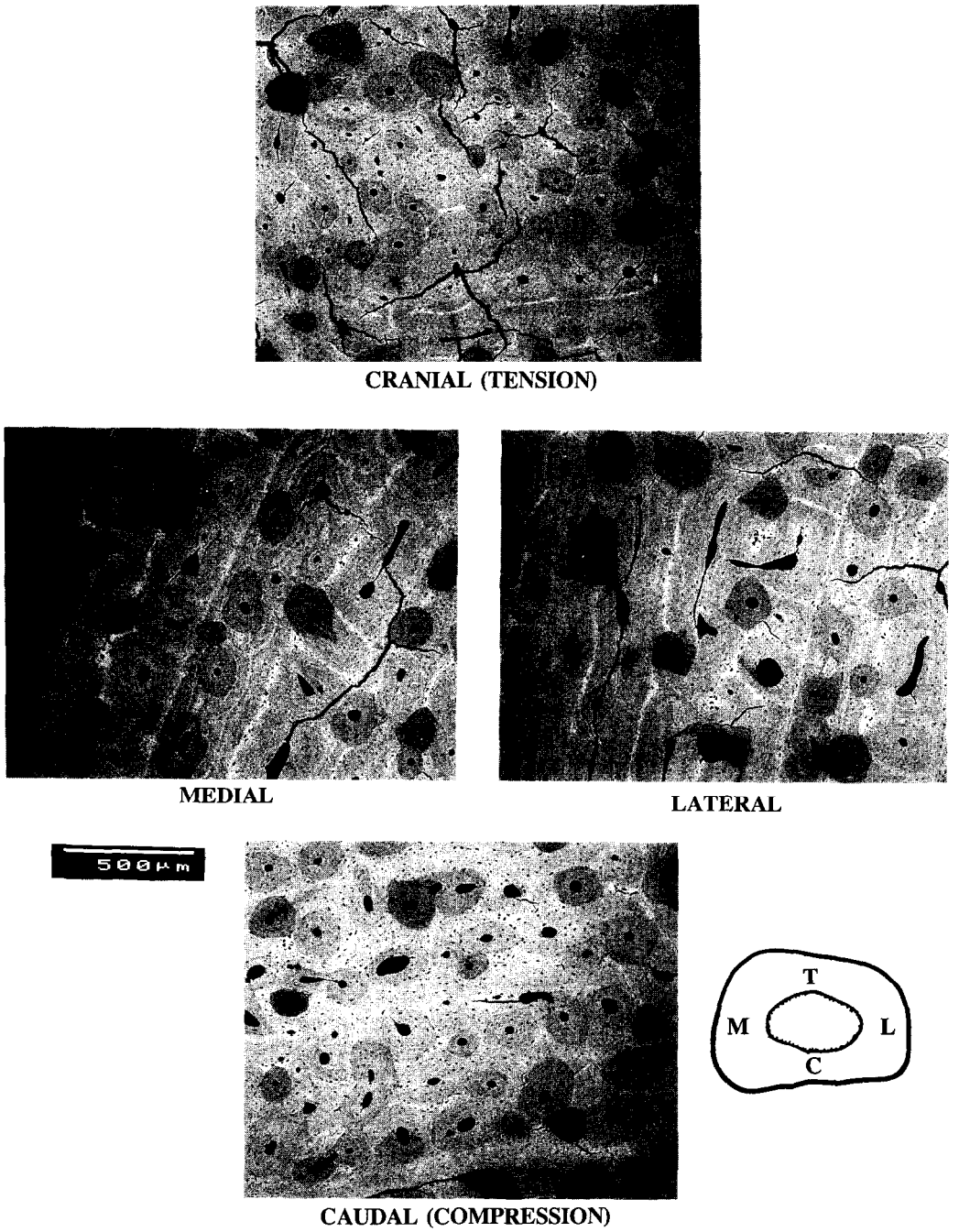

Figure 2. Representative backscattered electron micrographs from the middle envelope of each cortical region of a 50% section. In the diagram, T = cranial (tension), C = caudal (compression), M = medial, and L = lateral. Cracks in the specimens are artifacts of preparation and could not be avoided. Care was taken to exclude from the microstructure data the minimal effects that cracks might have on the data.[45] Original magnification 50×.

2.2%), the 50% sections (4.4 ± 2.5%) and the 65% sections (4.3 ± 2.2%) do not differ significantly ($p > 0.40$).

Mean area per osteon. Osteons in the caudal cortex (0.040 mm^2) of the 35% section are larger than osteons in any other region examined in this study, including the cranial cortex of the 35% sections (0.034 mm^2) (Table 2 and Figure 3d).

Collagen fiber orientation. Although the pattern of remodeled bone of the cranial and caudal cortices of the 35% sections is opposite that of the 50% and 65% sections, all sections had similar regional differences in collagen fiber orientation: the caudal cortex has relatively more oblique-to-transverse collagen fiber orientation, and the cranial cortex more longitudinal collagen fiber orientation ($p < 0.01$) (Table 3). The WMGLs between the medial and lateral regions do not significantly differ ($p > 0.4$)—which represents near-equivalent collagen fiber orientations between these opposing cortices. The WMGLs (collagen fiber orientation) of all envelopes in each cortex are also nearly the same (mean difference: 3.6%, $p > 0.4$).

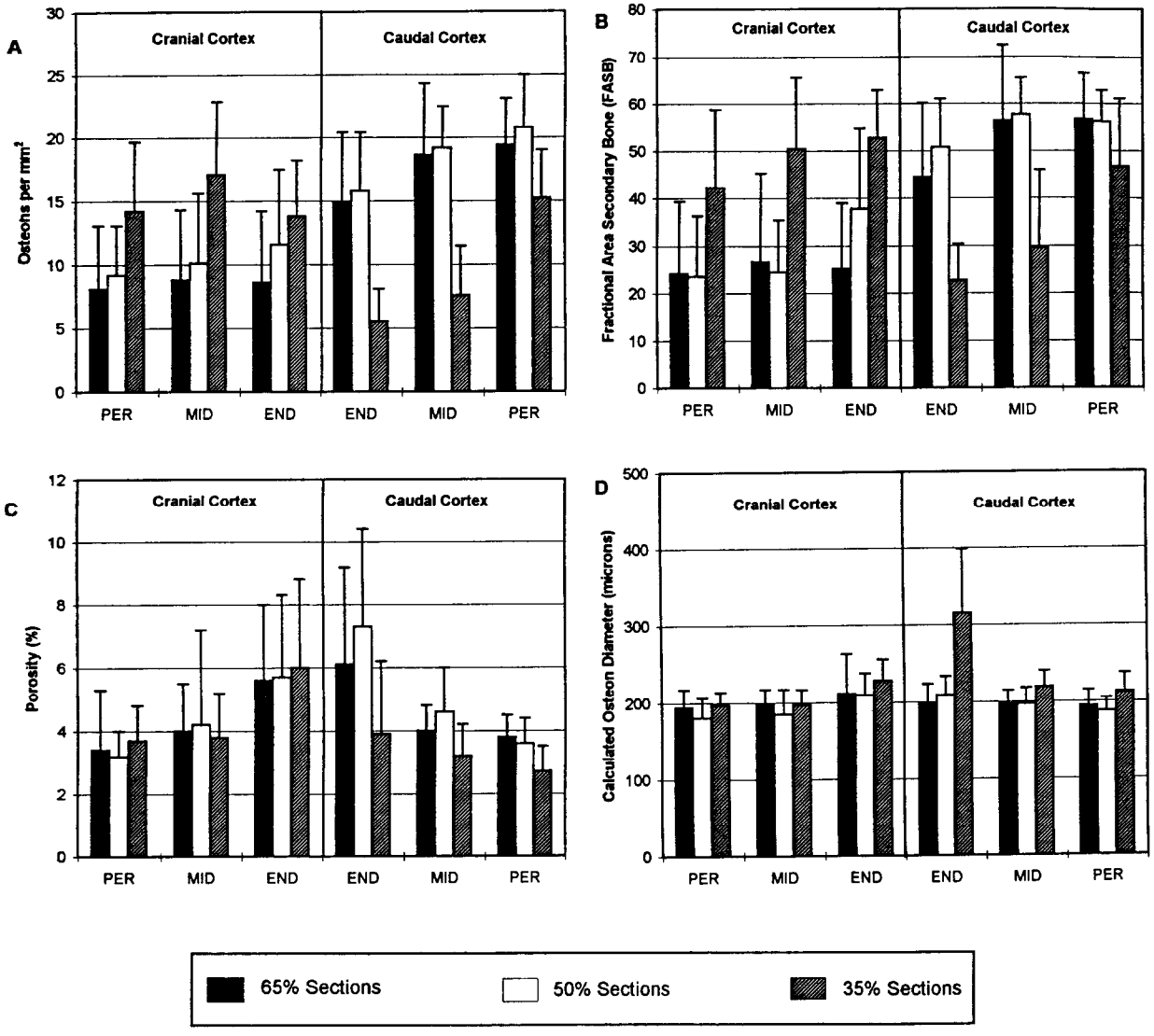

Figure 3. Graphic representation of microstructural data. (A) Osteon population density (number per square millimeter). (B) Fractional area of secondary bone (%). (C) Porosity (%). (D) Calculated osteon diameter (micrometers). PER = pericortical envelope; MID = middle envelope; END = endocortical envelope. Statistical probabilities of paired comparisons are reported in the text.

Discussion

Results of this quantitative study show, in the 50% and 65% sections, roughly twice as many osteons ($p < 0.01$) in the caudal (compression) cortex compared to the cranial (tension) cortex. The equal number of resorption spaces and uniform level of mineralization between the cranial and caudal cortices suggests that the formation of new secondary osteons (remodeling) was occurring at an equal rate between these regions at the time that these animals were collected. Comparison of the number of secondary osteons between the four cortical regions suggests that remodeling, at one time, occurred preferentially in regions loaded in compression. Several other bones that are habitually loaded in relatively unidirectional bending have been reported to have "compression" cortices that also have higher OPDs than the opposite "tension" cortices.[8,11,17,22–24,29,44,45] However, strain magnitudes are often greater in the compression cortex than in the tension cortex.[27] It is unclear whether the regional differences in OPDs are related to differences in strain magnitudes, strain modes, or some other feature(s) of the strain milieu.[15,22,27,36] It has been hypothesized that, during earlier stages of the maturation of a bone loaded in consistent bending, the more highly strained compression cortex would have sustained relatively more microdamage than the opposing tension cortex.[27,33,45] If this is true, then the increased OPD in the caudal cortex may simply represent regional differences in repair-mediated remodeling. However, to reject the hypothesis that strain mode is influential in these remodeling differences, it must be assumed that the lamellar constructs of osteons throughout a bone are consistently oriented with respect to the long axis of the bone. This assumption is challenged by the collagen orientation data reported in the present study of the standard breed horse radius and in other recent studies.[2,31,33,34] Osteons in the caudal cortex of the mid-to-proximal horse radius have secondary osteons with collagen fiber orientation that markedly differs from the collagen fiber orientation of the secondary osteons in the cranial, medial, and lateral cortical regions of the same transverse section. These data clearly raise the possibility that the

Bone Vol. 17, No. 3
September 1995:229–237

BMUs that are responsible for the construction of the secondary osteons in cranial and caudal cortices of the horse radius recognize the presence of strain mode.

An alternative hypothesis is that the orientations of the secondary osteons, not the fibers within them, differ between the cranial and caudal cortices of the horse radius. Based on observations of both osteon orientations and collagen fiber orientations in sagittal sections of the cranial and caudal cortices of the horse radius, Riggs et al.[33] concluded that the osteon orientations in these regions are closely aligned to the longitudinal axis of the bone. Therefore, they suggest that the small deviations (approximately 8°) from the longitudinal axis would not be of sufficient magnitude to significantly affect the intensity of transmitted light through thin sections of bone viewed under CPL. This suggestion is reinforced by data of Black et al.[6] showing that a deviation of greater than 25° would be required to cause a significant alteration in polarized transmitted light.

Riggs et al.[33,34] showed that, in transverse sections of the mid-diaphyses of radii of young skeletally immature thoroughbred and mixed breed horses, the primary bone (prior to remodeling) had collagen with predominantly longitudinal orientation, but that remodeled bone in the caudal cortex of more mature horses has predominantly oblique-to-transverse orientation. In contrast, they showed that remodeling in the cranial cortex not only produced fewer secondary osteons, but that the collagen fiber orientation within these osteons maintains the longitudinal orientation of the antecedent primary bone. Results of the present study therefore not only corroborate their findings, but also advance this line of inquiry by quantifying both the OPDs and collagen fiber orientations in the medial and lateral cortices of cortical regions and intracortical envelopes at several diaphyseal locations.

It has also been suggested that regional differences in OPD may be a remnant of cortical drift which occurs during growth.[1,15] The progressive decrease in OPD from the caudal pericortical envelope to the cranial pericortical envelope (Figure 3A) may be related to the progressive caudal-to-cranial remodeling of this cortex, which may occur subsequent to cortical drift of the diaphysis in this direction.[32] Although previous authors have ascribed transcortical variations in OPD to corresponding variations in strain magnitudes toward the neutral axis in accordance with Frost's flexion neutralization theory,[15,45] the fact that the OPD differences between envelopes of horse radius diaphysis do not exhibit this relationship suggests that these differences may be related to intracortical remodeling drifts. However, collagen fiber orientation does not exhibit this progressive caudal-to-cranial variation, but appears to be related to the strain mode that prevails within each cortex.

Cortical regions of the distal diaphyseal location were examined because loading conditions differ from those seen in the mid-to-proximal diaphysis.[41] The structural/material organization of the bone in this location is also more complex: cancellous bone fills the medullary canal and the cortices are thin (Figure 1). If regional OPD differences within the same transverse section actually represent adaptations that are related to the strain environment, then it is not surprising that the pattern of remodeled bone in the 35% location differs from that in the relatively more simply loaded proximal sections.

Structural/material analysis of the mule deer calcaneus,[44,45] a bone loaded in relatively simple and consistent cranial/caudal bending, suggests that other features of a bone's cortical organization may be more important than collagen fiber orientation in affecting a bone's regional material properties. The tension (caudal) cortex of the skeletally mature deer calcaneus is nearly completely remodeled with secondary osteons, and has multiple secondary osteon fragments, young secondary osteons, greater porosity, and more resorption spaces. This demonstrates that the secondary bone of this cortex is being more actively remodeled than other cortical regions of the same cross section.[45] If the primary objective of remodeling in the calcaneus is the realignment of collagen, then the observed active remodeling of bone in a region that had been previously highly remodeled with secondary osteons seems to serve no useful purpose, and may in fact weaken the bone by increasing porosity and decreasing mineral content.[12,26,45] In contrast, the tension cortex of the mature horse radius is incompletely remodeled, having relatively large amounts of primary bone. Differences between remodeling histories of the horse radius and the deer calcaneus suggest that the realignment of collagen may not be the sole objective of remodeling in all appendicular bones that are subject to habitual bending.

Tension and compression strains, produced by bending, represent 70% or more of the locomotion-induced longitudinal strains measured in the horse radius and in nearly all other limb bones that have been measured in vivo.[3,27] Strain modes may therefore be an important component of a signal that provides a cytologically beneficial stimulus to which bone cells are tuned for maintenance of mechanically competent tissue.[28,37,39] The presence of remodeling responses to regional differences in loading history, or absence of responses in some cases, of cortical bone may contribute to insuring some larger goal, such as the maintenance of adequate, or equal, safety-factors-to-failure in cortical regions throughout the volume of a bone.[24,34,44]

Although the data presented here may support the possibility that the BMUs produce the regionally heterogeneous tissue organization in response to prevailing strain modes, we emphasize that other unrecognized mechanical or nonmechanical factors may also be important.[28,39,45] Further, this work assumes a mechanical environment that may be oversimplified due to the lack of a rigorous rosette strain-gauge-based finite element analysis of the horse radius.[19] However, similarities between regional patterns of collagen fiber orientation in the diaphysis of the horse radius and regional patterns of collagen fiber orientation in other tension/compression bones suggest that the recognition of the strain mode component of a bone's internal strain milieu is an important factor in influencing the tissue organization of these bones.

Acknowledgments: This work was supported by the Department of Veterans Affairs Medical Research Funds, Salt Lake City, UT. We are grateful for the technical assistance of Peter Dirksmeier, Doug Ota, Cathy Sanderson, Gwenevere Shaw, Nikki Mihalopoulos, and Todd Parry.

References

1. Amprino, R. and Marotti, G. A topographic quantitative study of bone formation and reconstruction. Bone and Tooth: Proceedings of the First European Symposium; 1964; 21–33.
2. Ascenzi, A., Improta, S., Portigliatti Barbos, M., Carando, S., and Boyde, A. Distribution of lamellae in human femoral shafts deformed by bending with inferences on mechanical properties. Bone 8:319–325; 1987.
3. Biewener, A. A. Musculoskeletal design in relation to body size. J Biomech 24(suppl. 1):19–29; 1991.
4. Biewener, A. A., Swartz, S. M., and Bertram, J. E. A. Bone modeling during growth: Dynamic strain equilibrium in the chick tibiotarsus. Calcif Tissue Int 39:390–395; 1986.
5. Biewener, A. A., Thomason, J., Goodship, A., and Lanyon, L. E. Bone stress in the horse forelimb during locomotion at different gaits: A comparison of two experimental methods. J Biomech 16:565–576; 1983.

6. Black, J., Richardson, S. P., and Mattson, R. U. Haversian osteons: Longitudinal variation of internal structure. J Biomed Mater Res 14:41–53; 1980.
7. Bloebaum, R. D., Bachus, K. N., and Boyce, T. M. Backscattered electron imaging: The role in calcified tissue and implant analysis. J Biomater Appl 5:56–85; 1990.
8. Bouvier, M. and Hylander, W. L. Effect of bone strain on cortical bone structure in macaques (*Macaca mulatta*). J Morphol 167:1–12; 1981.
9. Boyce, T. M., Bloebaum, R. D., Bachus, K. N., and Skedros, J. G. Reproducible method for calibrating the backscattered electron signal for quantitative assessment of mineral content in bone. Scan Microsc 4:591–603; 1990.
10. Boyde, A. and Riggs, C. M. The quantitative study of the orientation of collagen in compact bone slices. Bone 11:35–39; 1990.
11. Carter, D. R., Caler, W. E., Spengler, D. M., and Frankel, V. H. Fatigue behavior of adult cortical bone: The influence of mean strain and strain range. Acta Orthop Scand 52:481–490; 1981.
12. Currey, J. D. The mechanical adaptations of bones. Princeton, NJ: Princeton University Press; 1984; 1–294.
13. Currey, J. D. and Hughes, S. M. The effects of pregnancy and lactation on some mechanical properties of the femora of the rat. Calcif Tissue Res 11: 112–123; 1973.
14. Emmanual, J., Hornbeck, C., and Bloebaum, R. D. A polymethyl methacrylate method for large specimens of mineralized bone with implants. Stain Technol 62:401–410; 1987.
15. Frost, H. M. Skeletal structural adaptations to mechanical usage (SATMU): 2. Redefining Wolff's Law: The remodeling problem. Anat Rec 226:414–422; 1990.
16. Getty, R. Sisson and Grossman's "The anatomy of the domestic animals." Philadelphia: Saunders; 1975.
17. Gies, A. A. and Carter, D. R. Experimental determination of whole long bone sectional properties. J Biomech 15:297–303; 1982.
18. Gross, T. S., McLeod, K. J., and Rubin, C. T. Strain energy density as a function of time: Characterizing the skeleton's functional strain history. Trans Orthopaed Res Soc 16:420; 1991.
19. Gross, T. S., McLeod, K. J., and Rubin, C. T. Characterizing bone strain distributions *in vivo* using three triple rosette strain gauges. J Biomech 25: 1081–1087; 1992.
20. Grynpas, M. Age and disease-related changes in the mineral of bone. Calcif Tissue Int 53(suppl. 1):S57–S64; 1993.
21. Lanyon, L. E. The success and failure of the adaptive response to functional load-bearing in averting bone fracture. Bone 13(suppl. 2):S17–S21; 1992.
22. Lanyon, L. E. and Baggott, D. C. Mechanical function as an influence on the structure and form of bone. J Bone Joint Surg 58-B:436–443; 1976.
23. Lanyon, L. E. and Bourn, S. The influence of mechanical function on the development and remodeling of the tibia: An experimental study in sheep. J Bone Joint Surg 61-A:263–273; 1979.
24. Lanyon, L. E., Magee, P. T., and Baggott, D. G. The relationship of functional stress and strain to the processes of bone remodeling: An experimental study on the sheep radius. J Biomech 12:593–600; 1979.
25. Marotti, G. Quantitative studies on bone reconstruction. 1. The reconstruction in homotypic shaft bones. Acta Anat 52:291–333; 1963.
26. Martin, B. Aging and strength of bone as a structural material. Calcif Tissue Int 53(suppl. 1):S34–S40; 1993.
27. Martin, R. B. and Burr, D. B. Structure, function and adaptation of compact bone. New York: Raven; 1989; 1–275.
28. Nelson, M. C., Skedros, J. G., Mason, M. W., and Bloebaum, R. D. Potential evidence of microstructural adaptation to specific strain features in cortical bone. Anat Rec (in press).
29. Nelson, M. C., Skedros, J. G., Mason, M. W., and Bloebaum, R. D. Potential evidence of microstructural, mineral, and cross-sectional adaptation to specific strain features in bone. Trans Orthopaed Res Soc 20:551; 1995.
30. Parfitt, A. M. Stereologic basis of bone histomorphometry: Theory of quantitative microscopy and reconstruction of the third dimension. In: Bone histomorphometry: Techniques and interpretation. Recker, R. R., ed. Boca Raton, FL: CRC; 1983; 53–88.
31. Portigliatti-Barbos, M., Bianco, P., Ascenzi, A., and Boyde, A. Collagen orientation in compact bone: II. Distribution of lamellae in the whole of the human femoral shaft with reference to its mechanical properties. Metab Bone Dis Rel Res 5:309–315; 1984.
32. Riggs, C. M., Lanyon, L. E., and Boyde, A. Preferred orientation of the ultrastructural elements of bone: Relationship with strain. Trans Orthopaed Res Soc 15:73; 1990.
33. Riggs, C. M., Lanyon, L. E., and Boyde, A. Functional associations between collagen fibre orientation and locomotor strain direction in cortical bone of the equine radius. Anat Embryol 187:231–238; 1993.
34. Riggs, C. M., Vaughan, L. C., Evans, G. P., Lanyon, L. E., and Boyde, A. Mechanical implications of collagen fibre orientation in cortical bone of the equine radius. Anat Embryol 187:239–248; 1993.
35. Rubin, C. T. and Lanyon, L. E. Limb mechanics as a function of speed and gait: A study of functional strains in the radius and tibia of horse and dog. J Exp Biol 101:187–211; 1982.
36. Rubin, C. T. and Lanyon, L. E. Regulation of bone mass by mechanical strain magnitude. Calcif Tissue Int 37:411–417; 1985.
37. Rubin, C. T. and McLeod, K. J. Biologic modulation of mechanical influences in bone remodeling. In: Biomechanics of diarthrodial joints. Mow, V. C., Ratcliffe, A., and Woo, S. L-Y., eds. New York: Springer; 1990; 97–118.
38. Rubin, C. T., McLeod, K. J., and Bain, S. D. Functional strains and cortical bone adaptation: Epigenetic assurance of skeletal integrity. J Biomech 23(suppl. 1):43–54; 1990.
39. Rubin, C. T., McLeod, K. J., Gross, T. S., and Donahue, H. J. Physical stimuli as potent determinants of bone morphology. Carlson, D. S. and Goldstein, S. A., eds. Bone biodynamics in orthodontic and orthopedic treatment. Ann Arbor, MI: University of Michigan Press; 1992; 75–91.
40. Russ, J. C. Practical stereology. New York: Plenum; 1986; 1–185.
41. Schneider, R. K., Milne, D. W., Gabel, A. A., Groom, J. J., and Bramlage, L. R. Multidirectional in vivo strain analysis of the equine radius and tibia during dynamic loading with and without a cast. Am J Vet Res 43:1541–1550; 1982.
42. Skedros, J. G., Bloebaum, R. D., Bachus, K. N., and Boyce, T. M. The meaning of graylevels in backscattered electron images of bone. J Biomed Mater Res 27:47–56; 1993.
43. Skedros, J. G., Bloebaum, R. D., Bachus, K. N., Boyce, T. M., and Constantz, B. Influence of mineral content and composition on graylevels in backscattered electron images of bone. J Biomed Mater Res 27:57–64; 1993.
44. Skedros, J. G., Bloebaum, R. D., Mason, M. W., and Bramble, D. M. Analysis of a tension/compression skeletal system: Possible strain-specific differences in the hierarchial organization of bone. Anat Rec 239:396–404; 1994.
45. Skedros, J. G., Mason, M. W., and Bloebaum, R. D. Differences in osteonal micromorphologies between tensile and compressive cortices of a bending skeletal system: Indications of potential strain-specific differences in bone microstructure. Anat Rec 239:405–413; 1994.
46. Turner, A. S., Mills, E. J., and Gabel, A. A. *In vivo* measurement of bone strain in the horse. Am J Vet Res 36:1573–1579; 1975.
47. Vigliani, F. Accrescimento e rinnovamento strutturale della compatta in ossa sottr. Tte alle sollecitazioni meccaniche. Zietschrift fur Zellforschung und Mikroskopische Anatomie Bd 42(S):59–76; 1955.

Date Received: March 16, 1995
Date Revised: May 25, 1995
Date Accepted: May 31, 1995